VOLUME 171 NUMBER 5 JUNE 2010

INTERNATIONAL JOURNAL OF PLANT SCIENCES

THE UNIVERSITY OF CHICAGO PRESS

Int. J. Plant Sci. 171(5):499–508. 2010.

1058-5893/2010/17105-0004$15.00 DOI: 10.1086/651947

MORPHOGENESIS IS HIGHLY ABERRANT IN THE VEGETATIVE BODY OF THE HOLOPARASITE *LOPHOPHYTUM LEANDRII* (BALANOPHORACEAE): ALL TYPICAL VEGETATIVE ORGANS ARE ABSENT AND MANY TISSUES ARE HIGHLY MODIFIED

Ana M. Gonzalez[1,*] and James D. Mauseth[2,†]

*Instituto de Botánica del Nordeste, Corrientes, W3402BKG, Argentina; and †Section of Integrative Biology, University of Texas, 1 University Station C0930, Austin, Texas 78712, U.S.A.

The vegetative body of *Lophophytum leandrii* is a "tuber" that completely lacks all vegetative organs typically found in photosynthetic plants. Tubers have a warty surface zone composed of parenchyma cells and brachysclereids; there is no epidermis. The interior of the tuber is a matrix of parenchyma cells and a ramified network of collateral vascular bundles. Ingrowths are abundant in vessels. Tubers grow diffusely by proliferation of parenchyma cells in the matrix and in vascular bundles and by a vascular cambium within each bundle. There are no apical meristems. The innermost portion of the surface zone is also a meristematic region, with warts enlarged by cell proliferation within their centers. The attachment point with *Parapiptadenia rigida* is a discrete woodrose: a "coralloid" interface caused by localized proliferation of host wood. Infection causes many changes in *P. rigida* wood development, most of which favor the success of the parasite. The only defensive reaction is that the host stops producing sieve tube members near the infection site. The woodrose and coralloid interface of *L. leandrii* seem to be intermediate between the simple interface of *Helosis*, and the elaborate chimeral interfaces of *Balanophora* and *Langsdorffia*.

Keywords: Balanophoraceae, Lophophytum, morphogenesis, organogenesis, parasitic plants.

Introduction

Molecular genetic studies of *Arabidopsis thaliana*, *Zea mays*, and other model species are advancing our understanding of plant morphogenesis (Doebley and Lukens 1998; Friedman et al. 2004; Alonso-Blanco et al. 2009), but developmental variability in most model species is not great (Barhélémy and Caraglio 2007). For example, all stems of all species consist of internodes and nodes with leaves and axillary buds: organogenesis is normal (i.e., what one would expect to find in a nonparasitic angiosperm). Furthermore, model plants have normal tissue development which produces epidermis, trichomes, guard cells, cortex, primary phloem and xylem (both of which always contain functional conducting cells), and pith (or conjunctive tissue in monocots); no model species lacks any of these cells or tissues, and none has them in unusual arrangements. Study of model plants alone cannot elucidate the plasticity or evolution of plant regulatory networks (Nardmann and Werr 2007).

As our theories of gene, cell, tissue, and organ interactions become more sophisticated, they should be extended to highly modified developmental systems such as, for example, the bodies of Cactaceae (Mauseth 2006) and Podostemaceae (Rutishauser 2000; Jäger-Zürn 2007; Koi and Kato 2007) and the vegetative bodies of holoparasitic plants (Heide-Jørgensen 2008). In many genera of holoparasitic plants, the vegetative portions appear to be released from many mechanisms that control normal organogenesis (Mauseth et al. 1984, 1985, 1992; Mauseth 1990; Mauseth and Montenegro 1992; Hsiao et al. 1993, 1994, 1995; Tennakoon et al. 2007). Depending on the species, the plants may have no roots, stems, leaves, nodes, or axillary buds. Many even lack epidermis, stomata, cuticle, root hairs, and endodermis. The vascular system in these taxa often is a set of irregularly branched vascular bundles embedded in a ground tissue that cannot properly be denoted as true cortex or pith. Inflorescence meristems must be produced as adventitious buds. Because holoparasitic plants evolved from more typical autotrophic ancestors (Der and Nickrent 2008; Judd et al. 2008), their highly modified morphogenic control mechanisms also must have evolved from those that control development in *Arabidopsis* and other model plants. Undoubtedly, both genes and transcriptional regulators have been highly modified (Doebley and Lukens 1998; Nardmann and Werr 2007).

Our knowledge of aberrant morphogenesis in holoparasitic plants is very incomplete because many genera have not been studied (Heide-Jørgensen 2008). We recently had the opportunity to collect samples of *Lophophytum leandrii* (fig. 1*A*, 1*B*), a holoparasite whose vegetative body is a subspherical subterranean mass covered by warts but lacking most typical plant parts. We report here our findings on the highly modified anatomy, growth, and morphogenesis of this species.

[1] Corresponding author; e-mail: anitama39@gmail.com.
[2] E-mail: j.mauseth@mail.utexas.edu.

Manuscript received December 2009; revised manuscript received February 2010.

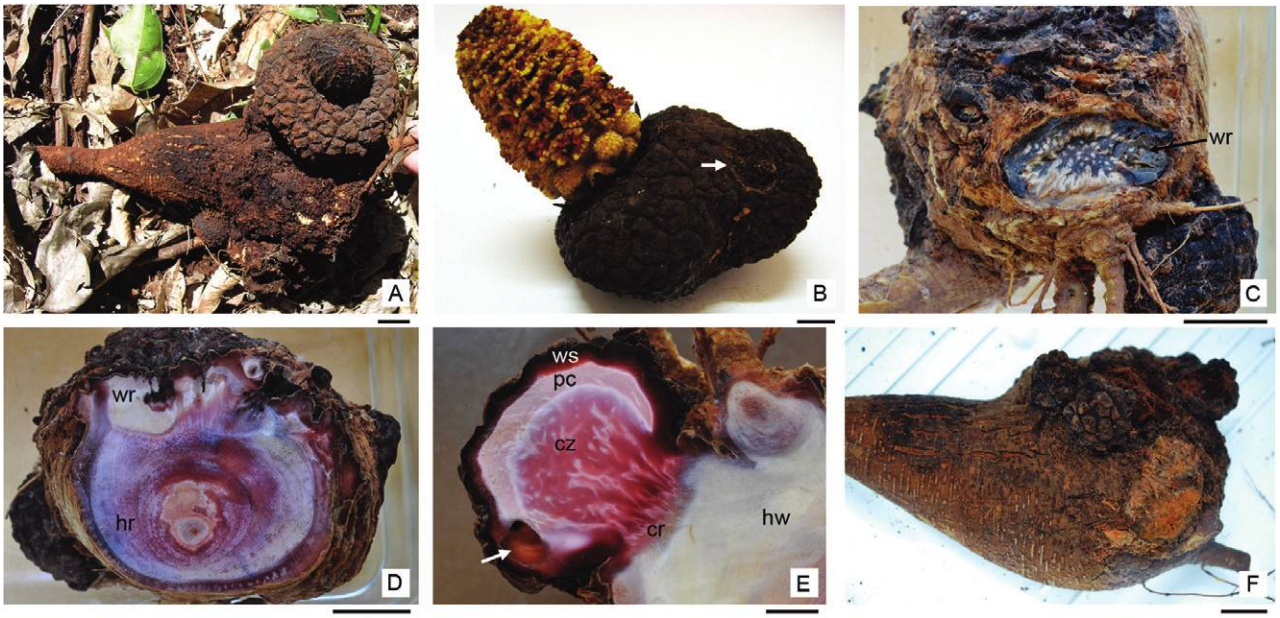

Fig. 1 Morphology of *Lophophytum leandrii* and *Parapiptadenia rigida*. *A*, Hypertrophied root of *P. rigida* with tuber and immature inflorescence of *L. leandrii*. Left, proximal uninfected, slender portion of the root; right, infected hypertrophied, club-shaped end of the root. A medium-size tuber of *L. leandrii* is present and bears an immature inflorescence. Note that the surface is extremely rough; this is due to many strands of *L. leandrii* running paradermally in the host secondary phloem, and also there are dozens of small nodules of *L. leandrii* cells. This same root is shown in lateral view in *F*. *B*, Tuber of *L. leandrii* with fully developed inflorescence; the arrow indicates the site where the tuber broke away from the host root when we collected it. *C*, Infected, hypertrophied root of *P. rigida* showing the host/parasite interface (*wr* = woodrose) in front view. The interface is visible because the *L. leandrii* tuber was pulled off, causing the host/parasite attachment to break at its weakest point, where host and parasite parenchyma met. *D*, Transverse section of host root (*hr*) at the zone of the woodrose. *E*, Longitudinal section through a small tuber showing warty surface zone (*ws*), narrow pale pink cap (*pc*), central vivid pink region (*cz*), coralloid interface (*cr*), and the host wood (*hw*); the region indicated by arrow shows the cavity where the inflorescence was developing (see fig. 2*M*). *F*, Lateral view of the hypertrophied, club-shaped root of *P. rigida* shown in *A*, after the large tuber was removed; on the left, the root tapers to its normal, uninfected diameter. The upper surface is the rough, disk-shaped patch in which strands of *L. leandrii* run paradermally through host secondary phloem. Several small tubers are visible, and hundreds of nodules are present between these tubers. Scale bars: *A*, *F*, 2 cm; *B*–*E*, 1 cm.

Material and Methods

Plants of *Lophophytum leandrii* Eichler parasitizing roots of trees of *Parapiptadenia rigida* Benth. (Fabaceae) were collected on Colonia Aborígen Andresito, San Ignacio, Misiones, Argentina, 27°15′32″S and 55°31′9″W. This tree is common in the Paranaense forest and reaches a height of up to 30 m. Voucher specimens, *L. leandrii* (Gonzalez, AM 246) and *P. rigida* (Gonzalez, AM 245) were deposited in the herbarium of Instituto de Botánica del Nordeste (CTES).

Plants of *L. leandrii* in different stages of development were collected and fixed in FAA (formaldehyde, acetic acid, 70% alcohol; 5 : 5 : 90). Infected and uninfected roots of *P. rigida* were also collected and fixed. Material was stored in FAA for several weeks or months, dissected, dehydrated through standard tertiary butyl alcohol series (Johansen 1940), and then embedded in Paraplast Plus. Sections were cut at 10–12 μm and then stained with a safranin–Fast Green combination (Mauseth et al. 1984). Histochemical tests included the IKI-H_2SO_4 method for tannins (Jensen 1962), phloroglucinol for cellulose/lignin, Sudan IV for fats, and $FeSO_4$ for tannins (Ruzin 1999). Starch grains were observed with polarized light or stained with iodine–potassium iodide (Johansen 1940).

Results

General Description of Plants of Lophophytum leandrii

Plants of *L. leandrii* consisted of a vegetative body or "tuber" that was subspherical or slightly flattened (fig. 1*A*, 1*B*). Tubers ranged in size from less than 1.0 mm in diameter when first visible emerging from host roots, up to 32 cm × 38 cm × 12 cm (the largest we encountered). All tubers were growing on roots (fig. 1*A*, 1*F*) close to the trunk of *Parapiptadenia rigida*, at a depth of 5.0 to 8.0 cm in the soil; only mature inflorescences emerged above soil level. Usually four to six tubers were found on the same tree.

Tubers bore no scales or leaves of any sort but were covered by polygonal or hexagonal "warts" of widths ranging from 0.3 to 1.2 cm. Tubers had no apex and no regions that resembled shoot or root apical meristems; there were no branches, runners, or roots emerging from the tubers, only a single inflorescence from larger tubers (fig. 1*B*). No tuber gave rise to a second tuber. Each tuber was connected directly to its host root at just a single point on the tuber's side or base but never its top; there was no stalk (fig. 1*B*). The connection was never larger than 4.8 cm in diameter, even in the largest tuber, and it

was fragile: tubers often broke away from the host root while being excavated. The attachment point was a small "woodrose," a small concave depression in the host tissue matched by conical haustorial tissue in the parasite (fig. 1*C*). The host/parasite interface in the woodrose was an irregular, "coralloid" set of radially oriented ridges and knobs caused by localized proliferation of host wood in the ridges and knobs and by lack of wood formation in the depressions (fig. 1*D*).

Tubers larger than 2.0 cm diameter each bore a single emergent inflorescence, with small tubers having an inflorescence bud (fig. 1*A*), larger tubers each having one mature inflorescence (fig. 1*B*). The smallest tuber with a mature inflorescence and open flowers was 6.0 cm in diameter. Inflorescence primordia formed internally (fig. 1*E*) then emerged through the upper side of the tuber; they never emerged through the bottom or sides of the tuber. Immature inflorescences were completely covered by black scales, but these fell away as the flowers matured acropetally.

Several collecting trips were made between May and September 2009. Plants of *L. leandrii* were located by searching around trees of *P. rigida*. In May, we encountered old dry inflorescences from the previous year, and on excavation, we found tubers with inflorescence buds only 3.0–4.0 cm tall, still subterranean. In June the inflorescences were still hidden beneath the dense leaf litter. In July and August, inflorescences had emerged and were visible, and flowers were open in September. Also in September, new tubers no larger than 3.0 cm in diameter were discovered, some already with small inflorescence buds visible without dissection.

Detailed Description of Plants of L. leandrii

When cut open, each tuber consisted of an outermost warty surface zone, completely black in color, and an interior body consisting of two parts: a central region of vivid pink matrix with white vascular bundles and a narrow pale zone (also with vascular bundles) between the central region and the warty surface zone (fig. 1*E*). These were the natural colors present in living healthy tubers.

Warty surface zone. The tuber's surface zone was 2.0–2.6 mm thick, being thinner in younger tubers and thicker in older ones. The surface matrix consisted of polygonal parenchyma cells ($\sim 80 \times 100$ μm) with thin walls and without obvious intercellular spaces (fig. 2*A*). The cytoplasm was extremely tanniniferous: it stained dark red with safranin and black with $FeSO_4$. No nuclei, starch grains, or other organelles were observed through the dense staining (fig. 2*B*). Brachysclereids (55–97 μm in diameter) were dispersed among the parenchyma cells of the surface zone (fig. 2*B*). They were solitary in young tubers, but in older tubers of medium size, they occurred in clusters with 4–10 sclereids visible in section and up to 45 sclereids visible per section in the largest tubers (fig. 2*A*, 2*C*). Sclereid secondary walls were 9.0–13 μm thick, composed of distinctive layers and numerous broad simple pits. Just as the parenchyma cells, the lumen of the brachysclereids were stained heavily due to tanninlike substances. The surface zone contained no vascular tissue.

The surface zone of large, old tubers was only slightly thicker than that of younger tubers but had much greater surface area, more cells, and many more warts. The innermost portion of the surface zone had features of a meristematic region: cells were smaller and stained less dark by safranin, and nuclei were visible (fig. 2*D*). No mitotic figures were seen, but the position and orientation of cell walls were consistent with cell division in this region. Immature brachysclereids with partially thickened, unlignified walls were encountered in this innermost meristematic region of the surface zone (fig. 2*D*). Just exterior to this meristematic zone, the parenchyma cells were larger and stained dark. Mature brachysclereids were present, either alone or in small clusters. The most superficial region of the surface zone was not a smooth layer of cells and did not resemble an epidermis: there was no cuticle, and there were no stomata or trichomes (fig. 2*A*). Instead, the matrix parenchyma cells at the surface were frequently broken or loosened, and both parenchyma cells and brachysclereids were being sloughed off (fig. 2*A*, 2*C*). Brachysclereids near the surface contained fungal hyphae, and their secondary walls were extensively digested by the fungi (fig. 2*E*). However, no fungi were seen in the adjacent parenchyma cells.

The surface zone was deeply cracked at the edges of warts, indicating that surface zone cells did not enlarge enough to compensate for growth of the tuber tissues below (fig. 2*C*). The warts themselves enlarged by cell proliferation within their centers. Cells in the center of warts stained less intensely than other parts of the surface layer, and cell wall patterns indicated that the cells had proliferated, pushing overlying cells into a wartlike shape. In young tubers, sclereids were especially sparse and mostly solitary as if proliferation of parenchyma cells had pushed existing sclereids (derived from the meristematic zone) away from each other. In older tubers, sclereids were much more abundant and occurred in large clusters separated by as few as 2–6 parenchyma cells. Apparently, parenchyma cells in the central regions of each wart had undergone proliferation, and then some of those cells adjacent to brachysclereid clusters converted themselves into sclereids, causing each cluster to become larger (fig. 2*F*).

Because old large tubers had more warts than young small tubers, new warts must have formed as tubers enlarged. When tubers were viewed from outside, many warts occurred in clusters that appeared to have been formed by the subdivision of preexisting warts.

Interior body of L. leandrii *tubers*. All tissues interior to the surface zone are being called here the "interior body." When a fresh tuber (either young and small, or old and large) was cut open, two regions were visible: a central vivid pink region and an outer cap that was pale pink (fig. 1*E*). These colors were still present in our oldest samples, which were stored in FAA for 7 mo. However, if tubers were cut open and the interior body was exposed to FAA, the surfaces became a uniform tan color and zonation disappeared. In fixed, embedded and stained sections, the two regions were sharply distinguished by the contents of the parenchyma cells: those in the outer cap contained numerous small dark red particles, whereas parenchyma cells in the central region had very smooth contents that stained various colors ranging from gray to red to purple, all in the same section (fig. 2*G*). In freehand sections, the central region showed a strong positive reaction for tannin with the ferrous sulfate method. The smoothness revealed the presence of amyloplasts (stained with IKI and confirmed by polarized light and presence of a hilum) and

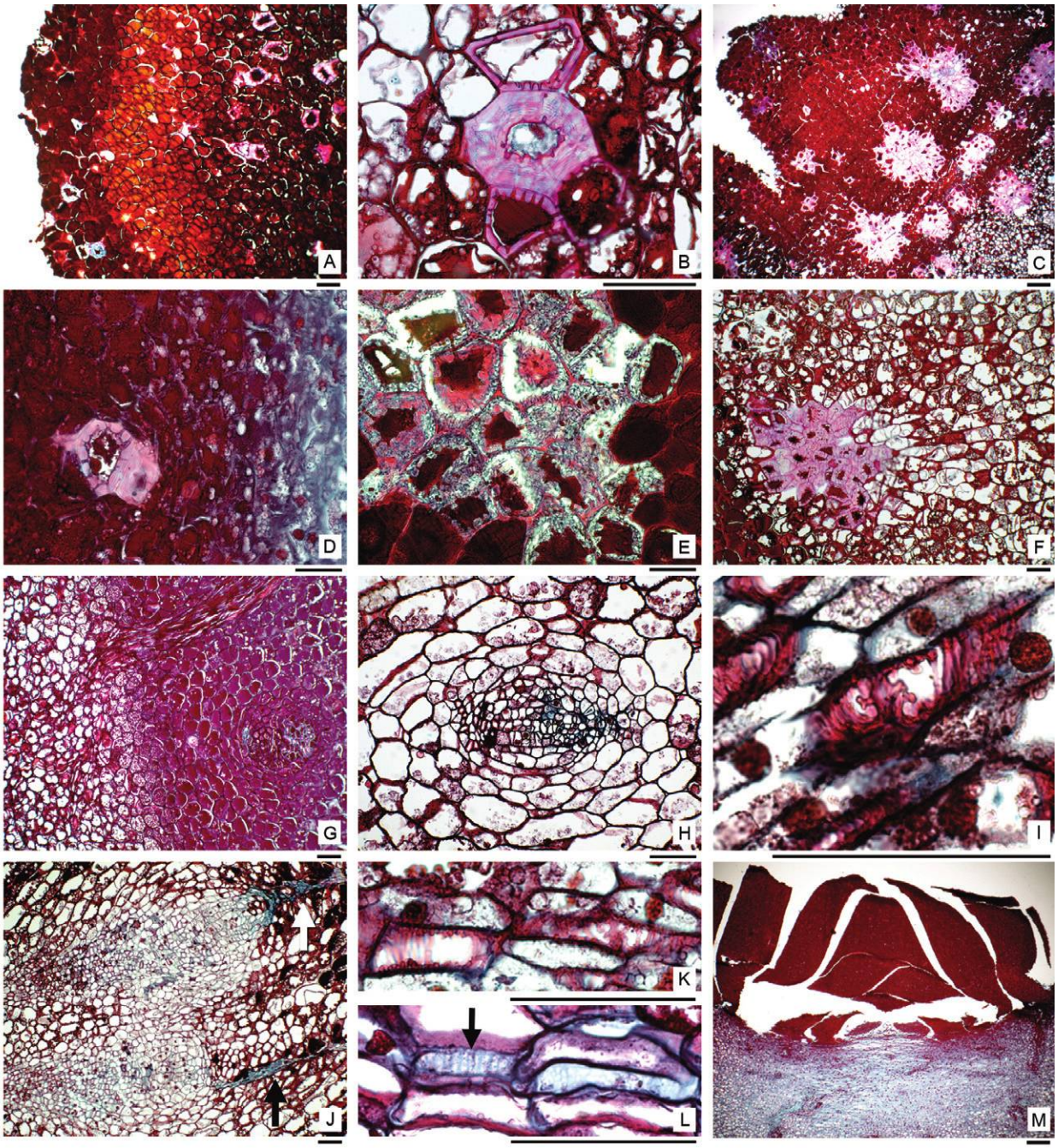

Fig. 2 Anatomical structures of *Lophophytum leandrii* tubers. *A*, The warty surface zone of a young tuber showing sparse groups of brachysclereids; the light zone in the center of the wart corresponds to the proliferated parenchyma cells. *B*, Mature and immature brachysclereids and matrix parenchyma cells in a surface wart. Note the abundant dark-stained tannins of most cells. *C*, Surface zone of large tuber; brachysclereids are in large clusters surrounded by tanniniferous parenchyma cells. The cleft on the left indicates the tuber's growth in volume causes its surface to split between warts. *D*, Innermost meristematic region of the warty surface is on the right side of the image. Immature sclereids are present. *E*, Clusters of brachysclereids invaded by fungal hyphae. Note the hyphae are digesting the cell walls but do not appear to be in the parenchyma cells. *F*, Detail of central region of a wart. Note the radiating pattern of cells, indicating the pattern of cell proliferation; centralmost cells have converted to a large cluster of brachysclereids. *G*, Interior body showing the vivid (right) and pale regions (left) of the tuber. Note the vascular bundle running through both zones and a second bundle inside the inner vivid zone. *H*, Cross section of collateral vascular bundle surrounded by a sheath in a *L. leandrii* tuber. *I*, Detail of *L. leandrii* vessels with wall ingrowths. Xylem parenchyma cells have large nuclei (almost 20 μm in diameter). *J*, Transverse section of two vascular bundles, each with a long strip of collapsed phloem (arrows). *K*, Longitudinal section of vascular bundle showing the xylem. *L*, Longitudinal section of phloem and healthy sieve tube members with sieve areas (arrow). *M*, Longitudinal section through a young inflorescence which had produced only scales at the time of dissection. This is located in a tuber cavity, as in figure 1*F*. Scale bars: *A*, *B*, *D–L*, 100 μm. *C*, *M*, 0.25 mm.

other spherical bodies of wax or fats (stained with Sudan IV; were not birefringent in polarized light and did not have a hilum). Starch grains were sparse in the pale pink outer cap, and no waxlike spheres were seen at all. Vascular bundles occurred in both regions of the interior body, and many were continuous from one region to the other. Brachysclereids occurred occasionally in the outer region of the outer cap but were never seen in the vivid pink central region. The volume of the central region was correlated with tuber volume: it was large in large tubers and small in small tubers, whereas the pale pink outer cap was thin in both (0.8–2.0 mm in small tubers; 6.0–10 mm in large tubers).

Vascular bundles were always collateral in both regions of the inner body (fig. 2*H*), and they ramified abundantly but never entered the surface zone. They were not organized in a single ring (a eustele), but in the most peripheral bundles, phloem was located on the outer side of each bundle (the side closer to the tuber surface). Vascular bundles contained thick-walled vessel elements with scalariform pitting that had ingrowths (fig. 2*I*). Ingrowths were abundant and easily visible in most vessels and sparse but still recognizable in a few. Perforation plates were simple. Almost every vessel lumen was filled with a substance that stained dark blue-violet; only rarely did we see vessels with clear, apparently empty lumens. The xylem in all bundles contained abundant parenchyma cells, all with extremely large nuclei (16.3 μm, SD 3.4 μm; fig. 2*I*, 2*K*). In most bundles, phloem was most easily recognized as long slender regions of collapsed cells that stained light blue compared to the dark red or violet of surrounding matrix cells (fig. 2*J*). Sieve tube members with sieve areas were seen only rarely—only if a sieve tube was cut in longitudinal section revealing compound sieve plates on a side wall (fig. 2*L*). Because of the irregular course of vascular bundles, few were cut in perfect transverse section, and in most of those, only a small amount of noncollapsed phloem was present; but in several fortuitous sections, sieve tube member/companion cell pairs were easily visible, with companion cells being slightly larger than sieve tubes and sieve tubes having a clear, unstained lumen (fig. 2*L*).

Most vascular bundles had two types of cell proliferation. Almost every bundle (even in medium-size tubers) had a vascular cambium that had produced large amounts of secondary phloem, most of which had collapsed into a thin long strip (fig. 2*J*). Secondary xylem was present but not nearly as abundant. Almost all vascular bundles were surrounded by a sheath of many layers of parenchyma cells that had the same orientation as the conducting cells and that appeared to have been produced by division of vascular parenchyma (fig. 2*H*, 2*J*). The long slender bands of collapsed phloem indicated that as the conducting cells collapsed, surrounding phloem parenchyma cells proliferated, pushing the earliest-formed phloem far away from the vascular cambium.

Inflorescence meristem. Small tubers ~2.0 cm in diameter, formed at the beginning of spring (September), contained a hollow cavity in their interior body, in either an apical or a lateral location and always on the border between the central region of vivid pink and the outer cap of pale pink cells (fig. 1*E*). In all our samples of these small tubers, the cavity contained a single inflorescence apical meristem, but unfortunately, the meristematic cells were collapsed. In small tubers, the meristem had produced only some inflorescence scales (fig. 2*M*). The smallest tuber we encountered in which flower initiation had begun was ~6.0 cm in diameter, and the inflorescence was ~2.0 cm tall.

General Description of Roots of Parapiptadenia rigida

Normal, uninfected root. Normal, uninfected roots of *P. rigida* had diffuse porous wood with vessels in clusters of two to four (fig. 3*A*). Vessels were broad (mean diameter 145.4 μm, SD 22.6 μm) and sparse (23–24 vessels/mm^2). In vessel elements, perforations were simple, and pits were abundant, alternate, vestured, narrow, and occasionally ramified. The wood matrix was mostly gelatinous fibers with thick walls. There was vasicentric aliform parenchyma with lightly stained contents, some containing starch grains and others containing rhomboidal crystals. Some axial parenchyma cells were filled with densely stained tannins. Apotracheal parenchyma was scarce, occurring in bands only 1 or 2 cells thick. Rays were uni- or biseriate and homogeneous.

The phloem of normal, uninfected roots consisted of tangential strata of (*a*) sieve tube members and companion cells, (*b*) parenchyma cells with granular tanninlike contents, and (*c*) bands of crystalliferous cells and gelatinous fibers (fig. 3*B*). Rays were uni- or biseriate for their entire length. In nonconducting outer phloem, the sieve tube members had collapsed and rays were sinuous; axial parenchyma cells proliferated, enlarged and filled with tannins. Cork cambium produced layers of cork to the exterior and a variable number of layers of tanniniferous phelloderm to the interior (fig. 3*C*). Lenticels were present and lacked closing layers. The cork cambium and its derivatives were separated from the nonconducting phloem by a band (~7–8 cells thick) of brachysclereids and crystalliferous cells (fig. 3*C*). These *P. rigida* phloem sclereids were smaller than those in the surface zone of *L. leandrii*, being only 17–23 μm in diameter. Each crystalliferous cell contained a rhomboidal crystal 9.0–12 μm across.

Uninfected but hypertrophied roots. Infection by *L. leandrii* caused adjacent proximal portions of the host root to become radially enlarged and to have altered anatomy, even though we did not detect any parasite cells in this region. For example, in one of the largest roots we collected, the infected area had a diameter of 10 cm and this tapered gradually to the normal diameter (1.5 cm in diameter) of uninfected portions of the root, which were only ~15 cm proximal (fig. 1*A*, 1*F*). There were no growth rings in the normal part of the root, but being so narrow, it was probably no more than 3 yr old. In the infected portion of this same root, the innermost wood had normal anatomy, and there were no *L. leandrii* cells; consequently, this root must have been at least in its second year when infected, and this amount of hypertrophy had occurred within just 1 or 2 yr.

In the hypertrophied but uninfected region, vessels were relatively slender (diameter 28.6 μm, SD 10.1 μm) and they were much more abundant, 61–72 vessels/mm^2 (fig. 3*D*). The quantity of gelatinous fibers decreased also, and the wood matrix instead consisted mostly of elongate lignified parenchyma cells with dark-stained tannins. Crystalliferous cells were absent. Rays became extremely sparse and even absent in some areas. Hypertrophied portions of root were so hard we could not cut them with a knife; sawing was necessary.

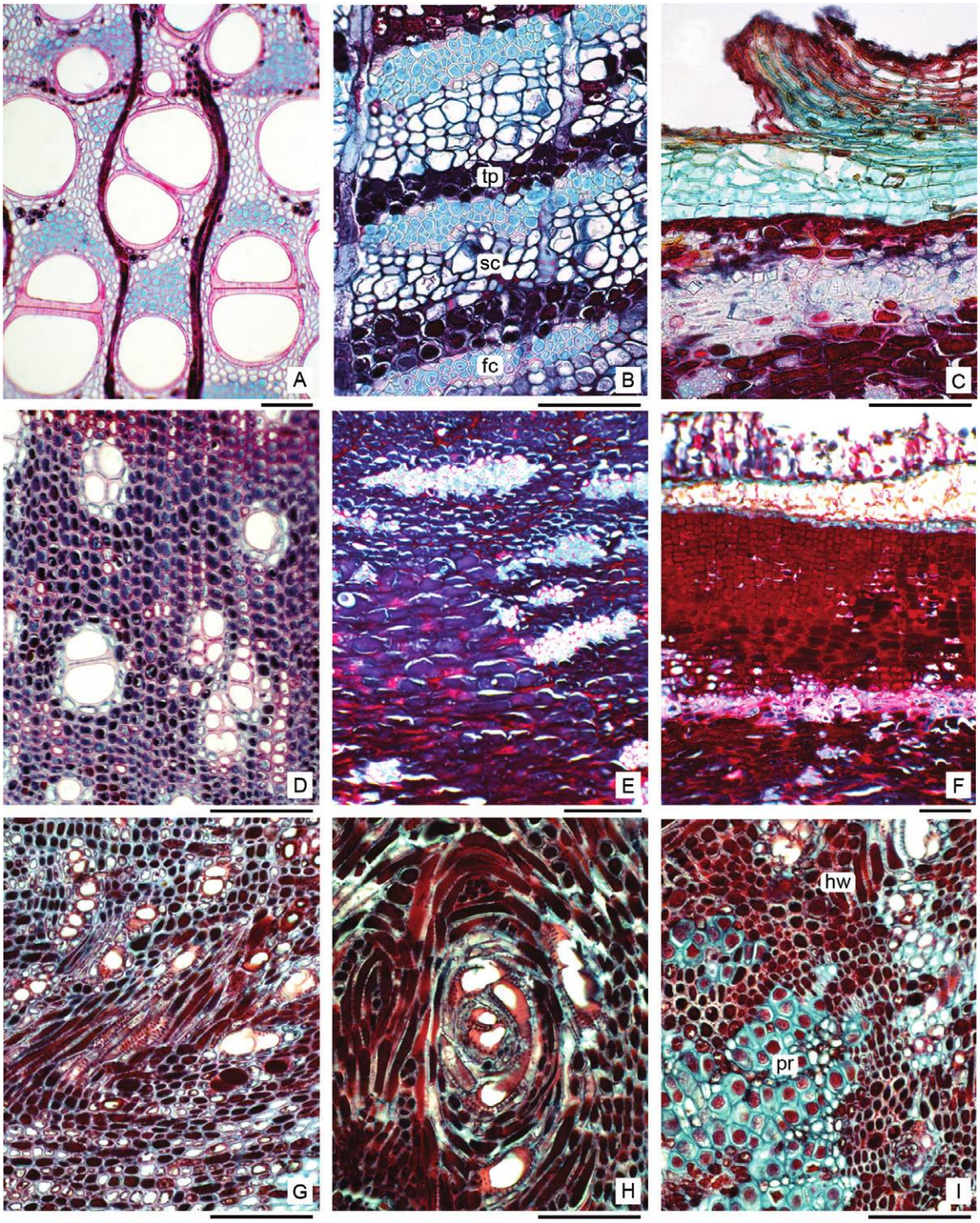

Fig. 3 Transverse sections of the root of *Parapiptadenia rigida*. *A*–*C*, Normal uninfected root. *A*, Diffuse porous wood with wide vessels, gelatinous fibers, and prominent rays. *B*, Functional secondary phloem showing bands of sieve tube members with companion cells (*sc*), tanniniferous parenchyma (*tp*), and gelatinous fibers intermixed with crystalliferous cells (*fc*). *C*, Periderm and nonfunctional phloem showing a band of sclereids and crystalliferous cells. The host sclereids are much smaller than *Lophophytum leandrii* sclereids (fig. 2*B*). *D*–*F*, Hypertrophied root proximal to infection (no parasite cells were found in this area). *D*, Affected wood; note the narrow vessels and the absence of rays. The matrix is lignified parenchyma, not fibers. *E*, Phloem showing the lack of tangential bands. No sieve tube members or companion cells were ever seen in this region. *F*, Outermost phloem (bottom) and periderm (top). *G*–*I*, Infected portions of the root. *G*, Xylem showing the change of direction of the elements. *H*, Concentric rings of vessels and lignified xylem parenchyma. *I*, Host wood (*hw*) intermixed with *L. leandrii* cells (*pr*, which are recognizable due to their very large nuclei). Scale bars: 100 μm.

In the hypertrophied but uninfected region, the phloem's tangential banding became disorganized, and phloem instead appeared to consist almost entirely of parenchyma cells with tannin contents with very few scattered fibers (fig. 3*E*). We did not detect any sieve tube members in this region: we did not see sieve areas or sieve plates, and in transverse section there were no empty cells nor pairs of cells that looked like sieve tube member/companion cell complexes. Although the vascular cambium continued to produce cells to its exterior, none seemed to be conducting cells. Lenticels were more abundant than in normal roots, and each had several closing layers (fig. 3*F*).

Infected regions of roots. The host root stopped elongation growth after infection and instead developed a broad, club-shaped end (fig. 1*A*). A large (14-cm diameter in one sample), irregular disk-shaped patch of the surface of the club-shaped end was extremely rough, and tubers of various sizes were present (fig. 1*F*). The roughness was primarily due to the presence of hundreds of tiny nodules (less than 1.0 mm in diameter) of *L. leandrii* cells located in the host secondary phloem and in outermost wood; many nodules had enlarged enough to distort the host's phloem and cork but not emerge from it. Several nodules were just large enough to have ruptured the cork and become visible to the naked eye, and two to five nodules were wider than 10 mm in diameter, but on any given root, only one at a time achieved a large size (more than 10 cm in diameter) and with an emergent inflorescence.

The nodules were interconnected by strands of *L. leandrii* running irregularly through the host phloem and spreading *L. leandrii* cells radially away from the site of initial infection (fig. 4*A*, 4*B*). These strands provided little host/parasite contact because they had a smooth surface with no interdigitations, they lacked vascular tissue, and their cells were filled with dark-stained material.

The host phloem under this disk-shaped patch was like that in the hypertrophied uninfected area described above: it had no detectable sieve tube members, few fibers, and instead was mostly just parenchyma cells filled with dark-stained material (fig. 4*B*). In this region, host wood anatomy was basically similar to that in the enlarged but uninfected area just proximal to this. Vessels were much narrower than in the center of the root (which had been formed before infection) and were more abundant (fig. 3*G*). Rays were almost completely absent as were fibers. Most of the infected wood consisted of lignified parenchyma cells that were filled with dark-stained contents and oriented radially (toward the tuber) rather than longitudinally. Many cells in infected host wood were oriented in concentric rings; these rings did not have *L. leandrii* cells at their centers (figs. 3*H*, 4*C*).

Initiation of L. leandrii *tubers/interface.* The different sizes of nodules on the infected club-shaped area represented different stages of tuber development. Strands of *L. leandrii*, while spreading through the host phloem, contacted host vascular cambium at numerous sites, infecting it. Host vascular cambium at these sites briefly remained active, producing large amounts of lignified parenchyma and narrower vessels. Very frequently, groups of *L. leandrii* cells were surrounded by new host wood cells (fig. 4*C*). Apparently some of the encased groups of parasite cells simply became trapped as more host wood was deposited exterior to them. Such nests of parasite cells (some moribund, some apparently healthy), were encountered at various depths of the infected hypertrophied wood (fig. 3*I*).

However, other nests of *L. leandrii* cells became meristematic instead and began to develop as nodules that would later become tubers (fig. 4*D*). The meristematic activity in these nodules produced matrix cells, tracheary elements, and surface cells. The surface in these tiny nodules had two regions and two very different fates: the surface cells at the outer portion of the nodule were in contact with host phloem, and those on the inner side were in contact with host vascular cambium. The portion of the nodule in direct contact with host phloem formed a surface layer of tanniniferous cells (but without warts while still located entirely within host tissues), and there seemed to be no means of absorbing material from host phloem (fig. 4*E*). There were no tracheary elements and no sieve elements in this part of the nodule surface; no cell appeared to be a transfer cell, and none appeared to be absorptive. Also, the host phloem in this contact zone appeared to lack conductive cells. Once tubers broke through the host root such that their own surface was exposed, they formed warts and at that point had all the zones of a mature tuber described above.

In contrast, the nodule surface in contact to the host vascular cambium formed an interdigitated structure that looked like coral in longitudinal sections (fig. 4*F*, 4*G*). Within the coralloid interface, cells of *L. leandrii* were meristematic (although no mitotic figures were seen in any sample) and had large nuclei (16.1–17.5 μm in diameter in cells that were only 17.5–22.3 μm wide by 29.0–33.3 μm long; fig. 4*H*).

The coralloid pattern increased in size and remained as the interface between the internal part of the tuber and the host xylem (fig. 4*F*). The *L. leandrii* meristematic cells formed fusiform groups only 2–4 cells long, surrounded on several sides by host cells (fig. 4*H*). The *L. leandrii* cells divided mostly transversely, producing at least short regions of orderly rows of cells, but overall, the tissues produced from this interface were irregular and calluslike. The derived cells matured quickly into either tanniniferous cells (the majority of the derivatives) or tracheary elements as parts of vascular bundles that extended uninterruptedly into the tuber. The tanniniferous cells were larger than the meristematic cells and were nucleate and stained dark (fig. 4*H*). The *L. leandrii* tracheary elements at the coralloid interface were short, polygonal, and irregular, with scalariform and reticulate walls (fig. 4*I*). Their secondary walls had ingrowths that made it possible to distinguish them from those of *P. rigida* (fig. 4*I*). The *L. leandrii* tracheary element lumens were filled with a dark-stained substance. Perforation plates were almost never seen near the coralloid interface, perhaps because they were absent or perhaps because of the dark-stained material in the elements. In several areas, direct contact between *L. leandrii* tracheary elements and host vessels was clearly visible (fig. 4*I*), although typically host and parasite vessels were separated by one or two meristematic cells (fig. 4*G*, 4*H*). Although all vascular bundles in the inner body of tubers contained phloem, we never saw an indication of any phloem at all in the coralloid contact area.

The *P. rigida* side of a coralloid interface also consisted of a narrow band of small cytoplasmic meristematic cells that could easily be distinguished from those of *L. leandrii* because

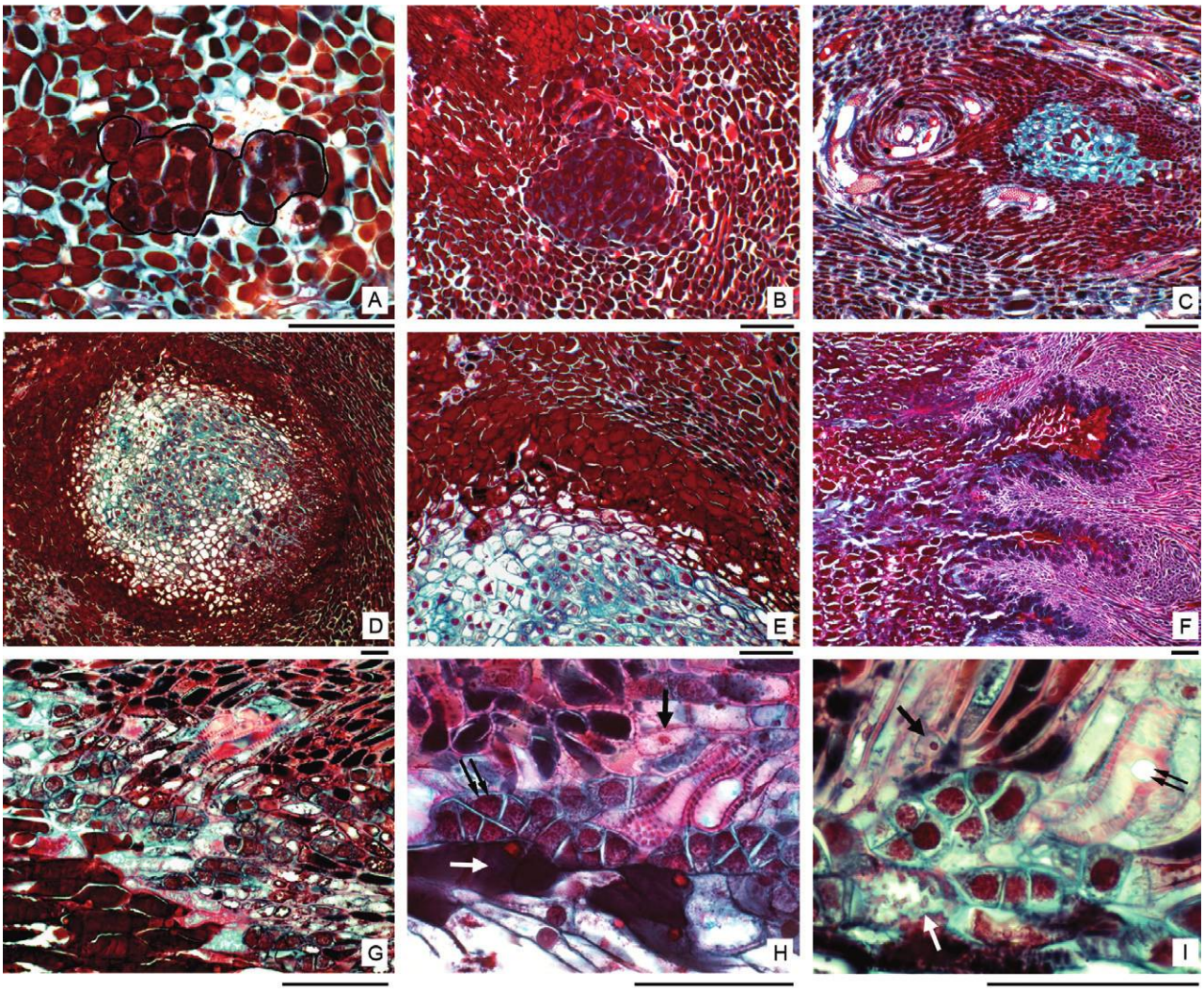

Fig. 4 *Lophophytum leandrii*/*Parapiptadenia rigida* interface (all photographs are transverse sections through root of *P. rigida*). *A*, *B*, Strands of *L. leandrii* cells inside host phloem. In *A* there is a line drawn around groups of parasite cells. *C*, Portion of host xylem invaded by *L. leandrii* meristematic cells; these will develop into nodules and then into tubers. *D*, Young nodule of *L. leandrii* inside host phloem; the lightly stained zone in the center contains the parasite matrix composed of parenchyma and vessels; the dark region surrounding it comprises the *L. leandrii*'s own tanniniferous surface cells. The edges of the image show host phloem. *E*, High magnification of *D*; note the absence of vascular connection between host phloem (upper part of the image) and parasite nodule. *F*, Coralloid interface, with host on right and parasite on left. *G*, Detail of coralloid interface; on the upper right is host wood, and on left bottom are tanniniferous parasite cells in coralloid interface. *H*, High magnification of the interface showing host parenchyma with small nuclei (single black arrow), tanniniferous parasite cells (white arrow), and meristematic parasite cells with large nuclei (double arrow). *I*, Another zone of the interface showing host parenchyma (single black arrow), host vessel with simple perforation plate (double arrow), and parasite tracheary element with wall ingrowths (white arrow). Scale bars: 100 μm.

they were much smaller and had smaller nuclei (fig. 4*H*). This band was only 2 or 3 cells thick, and immediately proximal to these cells were mature, elongate host wood parenchyma cells with slightly thickened lignified walls. Although no mitotic figures were seen, the small cytoplasmic cells must have produced the undulate, irregular coralloid interface pattern. Initiation of the coralloid interface caused host vascular cambium to stop functioning normally in that area, so only a small amount of more wood was produced there. But as the tuber enlarged, so did the coralloid portion of the contact area. Host cambial cells in contact with adjacent coralloid interface cells were recruited and acted as coralloid interface also. Host vascular cambium on the periphery of the contact area continued to produce secondary xylem and phloem, and consequently, the margins of the contact area were pushed outward as the host vascular cambium deposited wood to the inside. Because the center of the contact area did not move outward (because it had been converted to coralloid interface) as the tuber and interface aged, a concave woodrose formed.

Although some tubers we encountered were exceptionally large, many apparently had died and decomposed. Because most of the *L. leandrii* tuber was parenchyma, it decomposed almost completely, whereas *P. rigida*, being wood, remained as a woodrose. Large club-shaped roots typically bore several woodroses.

Discussion

The vegetative bodies of most holoparasitic plants differ greatly from those of autotrophic seed plants (Heide-Jørgensen 2008). Their highly modified bodies must be the result of highly modified processes of morphogenesis and development. Because heterotrophic plants must have evolved from autotrophic ancestors (Der and Nickrent 2008; Judd et al. 2008), it seems safe to assume that the genetic programs and regulatory networks that control morphogenesis in holoparasites evolved from those that control morphogenesis in normal plants. The morphogenesis of plants can be analyzed with respect to the initiation and development of organs, tissues, and cells.

Considering organs first, one principal characteristic of *Lophophytum leandrii* is the complete absence of all vegetative organs typically found in photosynthetic plants. The vegetative bodies of these holoparasites completely lack stems, roots, and leaves as well as apical meristems and axillary buds; this lack is especially significant because apical meristems and leaf primordia are critical components of regulatory networks in almost all plants (Friedman et al. 2004; Piazza et al. 2005; Nardmann and Werr 2007). In the evolution of the cactus family, there has been extreme reduction of leaves in many clades, but all still produce at least leaf primordia, presumably because they provide essential regulatory signals (Mauseth 2007). In vegetative bodies of *L. leandrii* and other members of Balanophoraceae (Moore 1940; Kuijt 1969; Hsiao et al. 1993, 1994; Heide-Jørgensen 2008), leaves are completely absent and all morphogenesis must occur without the signals they provide in normal plants.

In normal plants, root and shoot apical regions establish various layers of tissues within the developing body, and consequently they establish tissue patterns that are stereotyped in normal root and shoot (Steeves and Sussex 1989). The vegetative body of *L. leandrii* does have surface tissues and internal tissues, but because it lacks shoot and root apices, the spatial patterns of the tissues are not like those of a normal plant: there is no epidermis, no eustele, no protostele, no cortex, and no pith.

Considering now the initiation and morphogenesis of tissues rather than the organs, some aspects are normal, and others are highly modified. For example, the tuber surface possesses no epidermis at all. It has no epidermal cells, cuticle, waxes, trichomes, or stomata, and all aspects of epidermis are absent. Although there is no typical periderm, cork, or lenticels on *L. leandrii* tubers, the warty surface layer is produced by a meristematic zone at its innermost edge; it is possible that this evolved from a cork cambium whose derivates now mature into tanniniferous parenchyma and sclereids rather than into cork cells. The presence of tannins would offer protection against attack by pathogens and delay decomposition while in humid soils (Evert 2006).

The morphogenesis of vascular tissues of *L. leandrii* is much less modified than that of its surface tissues. The vascular bundles form in an unusual ramified three-dimensional network. This anomalous pattern is probably due to diffuse growth of ground parenchyma as well as the lack of apical meristems and leaf primordia, two tissues that are sources of morphogenetic signals that organize vascular tissues in normal plants (Reinhardt et al. 2003).

Also, mechanical signals that influence morphogenesis must be considered (Dumais 2009): rather than growing as a bipolar axis with two localized apical meristems, tubers of *L. leandrii* grow more or less isodiametrically by diffuse cell division in their ground and vascular tissues. They must experience very different growth stress than do normal plants.

Tissues within vascular bundles, however, show almost completely normal morphogenesis. All vascular bundles contain both xylem and phloem, and the phloem is basically normal, having sieve tube members, companion cells, and phloem parenchyma. The xylem has complete vessels and xylem parenchyma, the only detectable anomaly being the presence of wall ingrowths. The genes responsible for xylem and phloem differentiation must still be very similar to those of autotrophic plants and are capable of functioning normally despite the modifications in so many surrounding tissues. Vegetative bodies of *L. leandrii* also form vascular cambia, and these appear to have no obvious modifications. Once old enough, each vascular bundle produces a fascicular cambium that is bifacial and that continuously produces new secondary xylem and phloem. As in many species that produce only a small amount of wood (Mauseth 2006), no interfascicular cambium is formed. Many genes are already known to affect secondary growth (Groover and Robischon 2006), and they must still be functional in *L. leandrii*. The ground matrix of the tuber consists of parenchyma cells that appear to be completely normal, with the exception that they proliferate and are responsible for much of the growth of the tuber.

Natural selection has obviously acted extensively on the morphogenetic mechanisms that control the development of *L. leandrii*'s own body. It is reasonable to ask whether *L. leandrii* is able to exert control over the morphogenesis of its host. For example, *Balanophora* and *Langsdorffia* (both Balanophoraceae) induce the root tissue of the host to proliferate and grow into the tuber, such that the tuber body is a mix of both host and parasite cells (Kuijt 1969; Shivamurthy et al. 1981; Gedalovich-Shedletzky and Kuijt 1990; Hsiao et al. 1994). The tuber vascular bundles in both genera are chimeras that consist of host and parasite cells in very specific patterns. These elaborate chimeric bundles almost certainly indicate that the parasite has extensive control over host development. It is known that *Orobanche* is able to induce certain genes in its host (Joel and Portnoy 1998).

Host reactions in *Lophophytum* and *Parapiptadenia* are not nearly so elaborate, and only one host reaction seems to be defensive: the host stops producing sieve tube members and companion cells when *L. leandrii* infects it. All other host responses seem to favor the parasite: after infection the host produces vessels that are narrower and more similar in diameter to those of *L. leandrii*, host vascular cambium produces a wood matrix consisting of living parenchyma cells rather than dead fibers, and the zone of infection is better aerated because the of number of lenticels increases. Although natural selection is acting on both *Lophophytum* and *Parapiptadenia*, it appears that most modifications favor the success of the parasite.

Considering the extensive modification of the vegetative body of *L. leandrii*, it is important to point out that its inflorescences have normal organization with shoot meristems, epidermis, eustele, and so on (A. M. Gonzalez and J. D. Mauseth, unpublished manuscript). Genes for many aspects of

morphogenesis must be present and functional in the genome but are repressed or have altered expression in the vegetative body.

The Balanophoraceae would be a good family for studying many aspects of the evolution of morphogenetic mechanisms. The host/parasite interface is simple in *Helosis* (Hsiao et al. 1993), complex in *Balanophora* and *Langsdorffia* (Kuijt 1969; Shivamurthy et al. 1981; Gedalovich-Shedletzky and Kuijt 1990; Hsiao et al. 1994), and intermediate in *Dactylanthus* (Moore 1940) and *Lophophytum*. The vegetative bodies in the family vary greatly in complexity, and some genera produce a structure called a "runner" that can infect nearby host roots (e.g., in *Helosis* and *Ombrophytum*; Mauseth et al. 1992; Hsiao et al. 1993), whereas others have ramified tubers (as in *Langsdorffia*; Hsiao et al. 1994), and still others (*Lophophytum*) lack runners but can spread themselves within a host by means of strands in the host phloem. This family is rich in modifications and variations that can help us more fully understand plant morphogenesis.

Acknowledgments

This research was completed through a fellowship from the CONICET/Fulbright program for a postdoctoral fellowship (A. M. Gonzalez) and the University of Texas at Austin. We thank Dr. Popoff and the people of the indigenous community "Andresito" for help during collecting trips in Argentina. We thank Glenn Croft for his skillful assistance.

Literature Cited

Alonso-Blanco CM, GM Aarts, L Bentsink, JJB Keurentjes, M Reymond, D Vreugdenhil, M Koornneef 2009 What has natural variation taught us about plant development, physiology, and adaptation? Plant Cell 21:1877–1896.

Barhélémy D, Y Caraglio 2007 Plant architecture: a dynamic, multilevel and comprehensive approach to plant form, structure and ontogeny. Ann Bot 99:375–407.

Der JP, DL Nickrent 2008 A molecular phylogeny of Santalaceae (Santalales). Syst Bot 33:107–116.

Doebley J, L Lukens 1998 Transcriptional regulators and the evolution of plant form. Plant Cell 10:1075–1082.

Dumais J 2009 Plant morphogenesis: a role for mechanical signals. Curr Biol 19:207–208.

Evert RE 2006 Esau's plant anatomy, meristems, cells, and tissues of the plant body: their structure, function, and development. Wiley, New York.

Friedman WE, RC Moore, MD Purugganan 2004 The evolution of plant development. Am J Bot 91:1726–1741.

Gedalovich-Shedletzky E, J Kuijt 1990 An ultrastructural study of the tuber strands of *Balanophora* (Balanophoraceae). Can J Bot 68: 1271–1279.

Groover A, M Robischon 2006 Developmental mechanisms regulating secondary growth in woody plants. Curr Opin Plant Biol 9: 55–58.

Heide-Jørgensen HS 2008 Parasitic flowering plants. Brill, Leiden, Netherlands.

Hsiao SC, JD Mauseth, LD Gomez 1993 Growth and anatomy of the vegetative body of the parasitic angiosperm *Helosis cayennensis* (Balanophoraceae). Bull Torrey Bot Club 120:295–309.

——— 1994 Growth and anatomy of the vegetative body of the parasite angiosperm *Langsdorffia hypogaea* (Balanophoraceae). Bull Torrey Bot Club 121:24–39.

Hsiao SC, JD Mauseth, CI Peng 1995 Composite bundles, the host/parasite interface in the holoparasitic angiosperms *Langsdorffia* and *Balanophora* (Balanophoraceae). Am J Bot 82:81–91.

Jäger-Zürn I 2007 The shoot apex of Podostemaceae: de novo structure or reduction of the conventional type? Flora 202:383–394.

Jensen N 1962 Botanical histochemistry: principles and practices. WH Freeman, London.

Joel DM, VH Portnoy 1998 The angiospermous root parasite *Orobanche* L. (Orobanchaceae) induces expression of a pathogenesis related (PR) gene in susceptible tobacco roots. Ann Bot 81:779–781.

Johansen DA 1940 Plant microtechnique. McGraw-Hill, New York.

Judd WS, CS Campbell, EA Kellogg, PE Stevens, MJ Donoghue 2008 Plant systematics—a phylogenetic approach. Sinauer, Sunderland, MA.

Koi S, M Kato 2007 Developmental morphology of the shoot in *Weddellina squamulosa* and implications for shoot evolution in the Podostemaceae. Ann Bot 99:1121–1130.

Kuijt J 1969 The biology of parasitic flowering plants. University of California Press, Berkeley.

Mauseth JD 1990 Morphogenesis in a highly reduced plant: the endophyte of *Tristerix aphyllus* (Loranthaceae). Bot Gaz 151:348–353.

——— 2006 Structure-function relationships in highly modified shoots of Cactaceae. Ann Bot 98:901–926.

——— 2007 Tiny but complex foliage leaves occur in many "leafless" cacti. Int J Plant Sci 168:845–853.

Mauseth JD, SC Hsiao, G Montenegro 1992 Vegetative body of the parasitic angiosperm *Ombrophytum subterraneum* (Balanophoraceae). Bull Torrey Bot Club 119:407–417.

Mauseth JD, G Montenegro 1992 Secondary wall ingrowths on vessel elements in *Ombrophytum subterraneum* (Balanophoraceae). Am J Bot 79:456–458.

Mauseth JD, G Montenegro, AM Walckowiak 1984 Studies of the holoparasite *Tristerix aphyllus* (Loranthaceae) infecting *Trichocereus chilensis* (Cactaceae). Can J Bot 62:847–857.

——— 1985 Host infection and flower formation by the parasite *Tristerix aphyllus* (Loranthaceae). Can J Bot 63:567–581.

Moore LB 1940 The structure and life-history of the root parasite *Dactylanthus taylori* Hook f. N Z J Sci Technol B 21–22:206–224.

Nardmann J, W Werr 2007 The evolution of plant regulatory networks: what *Arabidopsis* cannot say for itself. Curr Opin Plant Biol 10:653–659.

Piazza P, S Jasinski, M Tsiantis 2005 Evolution of leaf developmental mechanisms. New Phytol 167:693–710.

Reinhardt D, ER Pesce, P Stieger, T Mandel, K Baltensperger, M Bennett, J Traas, J Friml, C Kuhlemeier 2003 Regulation of phyllotaxis by polar auxin transport. Nature 426:255–260.

Rutishauser R 2000 Developmental morphology of *Apinagia multibranchiata* (Podostemaceae) from the Venezuelan Guyanas. Bot J Linn Soc 132:299–323.

Ruzin SE 1999 Plant microtechnique and microscopy. Oxford University Press, New York.

Shivamurthy GR, GD Arekal, BGL Swamy 1981 Establishment, structure and morphology of the tuber of *Balanophora*. Ann Bot 47:735–745.

Steeves TA, IM Sussex 1989 Patterns in plant development. Cambridge University Press, Cambridge.

Tennakoon KU, JF Bolin, LJ Musselman, E Maass 2007 Structural attributes of the hypogeous holoparasite *Hydnora triceps* Drège & Meyer (Hydnoraceae). Am J Bot 94:1439–1449.